This is a peer-reviewed, author's accepted manuscript of the following conference output:
Alassi, A., Ahmed, K., Egea-Alvarez, A., & Foote, C. (2021). Modified grid-forming converter control for black-start and grid-synchronization applications.
In 2021 56th International Universities Power Engineering Conference (UPEC) (pp. 1-5). IEEE. https://doi.org/10.1109/upec50034.2021.9548162

Modified Grid-forming Converter Control for Black-Start and Grid-Synchronization Applications

Abdulrahman Alassi
Iberdrola Innovation Midde East &
University of Strathclyde
Doha, Qatar
aalassi@iberdrola.com

Khaled Ahmed & Agusti Egea-Alvarez
University of Strathclyde
Glasgow, United Kingdom
khaled.ahmed@strath.ac.uk
agusti.egea@strath.ac.uk

Colin Foote
ScottishPower Energy Networks
Glasgow, United Kingdom
cfoote@spenenergynetworks.co.uk

***Abstract*— The increasing grid integration of converter-based generation and distributed resources is necessitating a review to the classical synchronous generators dominant network models, and to equip converters with the necessary control capabilities such as inertia emulation and black-start to carry on the required ancillary services provision. This paper proposes a modified grid-forming converter control technique based on virtual synchronous machine (VSM). The modified controller uses a ramping voltage reference to achieve soft transformer energization and eliminate high-magnitude inrush current that can traditionally exceed converters rating. Grid-synchronizing functionality is added to the VSM controller to achieve smooth transition from black-start to grid-connected mode while maintaining grid-forming operation. This is achieved by gradually adjusting the power loop reference through a dedicated synchronizing controller, which is disconnected once grid-connection is achieved. A MATLAB/ Simulink case study is presented to illustrate the controller performance with a 40 MVA simulated converter. The results demonstrate successful black-start sequence execution, starting by soft transformer energization, followed by a block load pickup and grid-synchronization. The sequence is achieved with minimal transformer inrush current, and with seamless transition to the grid-connected operating mode.**

Keywords—grid forming converters, synchronization, black start, transformer energization, virtual synchronous machine.

I. Introduction

The use of grid-forming converters (GFC) in distribution networks is attracting more attention globally due to their prospective role in network and inertia support, and their wide array of ancillary services capabilities [1]. A GFC can establish a stable controlled voltage on its AC terminals without requiring an external reference such is the case for grid-following converters (GFL). This makes GFCs suitable to act as anchor generation units in black-start events.

GFC control can be achieved using different techniques, such as droop, power synchronizing control (PSC), dispatchable virtual oscillator (dVOC), virtual synchronous machine (VSM) … etc [2, 3]. The selection of a particular technique is influenced by the array of ancillary services required by the converter. Some controllers, for instance, can provide inertia support with mathematically analogous parameters to synchronous generators such as VSM [4]. GFCs control operates the converter in voltage and frequency (V/f) mode by producing controlled voltage and angle reference.

Black-start applications involve different steps, such as transformers and cable energizations, load pickup and grid synchronization. Transformer energization has long been a task associated to conventional synchronous generators (SG) as the dominant power source in public grids. As strong sources with high short-term overcurrent capabilities, SGs can typically withstand the inrush current requirements of a transformer that can be up to 7-10 times the nominal current [5]. On the other hand, power converters have very strict current limits for protection, which are typically limited to 1.5 p.u. and for very short time periods [6]. This means that the use of power converters for transformers energization is often linked to inrush current mitigation techniques. Given the converters voltage control flexibility, soft energization with a controlled voltage ramp has been proposed in several works for transformers inrush current mitigation [7, 8].

Once the voltage island is established, load pickup during black-start can be performed with bulk loads, or gradually in a successive manner to mitigate voltage disturbances at the point-of-common-coupling (PCC). Connecting large loads behind an impedance may lead to measurable voltage drop at the PCC, which can be mitigated in island operation by using transformers On-Load-Tap-Changers (OLTC) when present.

Synchronizing the restarted island to the grid is an important black-start step to group different neighboring electrical islands and/or to achieve synchronized operation with the grid. This requires the matching of voltage amplitude, frequency, and phase between the synchronized segments prior to closing circuit breakers. For GFCs case, the outer grid-forming control loop should adjust its power loop angle to sync with the grid voltage angle. Literature is constantly updated with new papers to propose modified GFCs grid synchronization techniques, particularly for voltage angle and frequency, aiming to achieve improved performance [9, 10]. Grid and GFC sides voltage angles can be measured using phase-locked-loops (PLLs) or Fourier transformations, the former provides information on the three phases whereas the latter provides information on individual phases. Then, the difference between both sides voltage angles is typically passed to a controller, such as proportional integral (PI) to drive it to zero prior to synchronization. The controller can either drive the angle directly [10], or adjust the converter power reference [11].

Black-start has been known to be an ancillary service that can be provided by voltage source converters (VSC) in applications such as HVDC [12]. The increased Distributed Energy Resources (DER) penetration in distribution networks is putting this ancillary service under research spotlight again in Medium Voltage (MV) distribution networks context. Various international collaborations are currently testing this functionality on an industrial scale such as the Distributed ReStart project in the UK [13]. Similar efforts are made by a range of technology manufacturers to provide software and/or hardware upgrades to their converters.

The system configuration for a black-start of a network from DERs relies on several factor such as the number of compatible present DERs and circuits routing. In this paper, it is assumed that a single GFC is connected to large battery system as the black-start DER. The GFC is interfaced to a saturable distribution transformer that it should energize. Load banks and grid breakers are connected at the PCC. The considered system is graphically illustrated in Fig. 1.

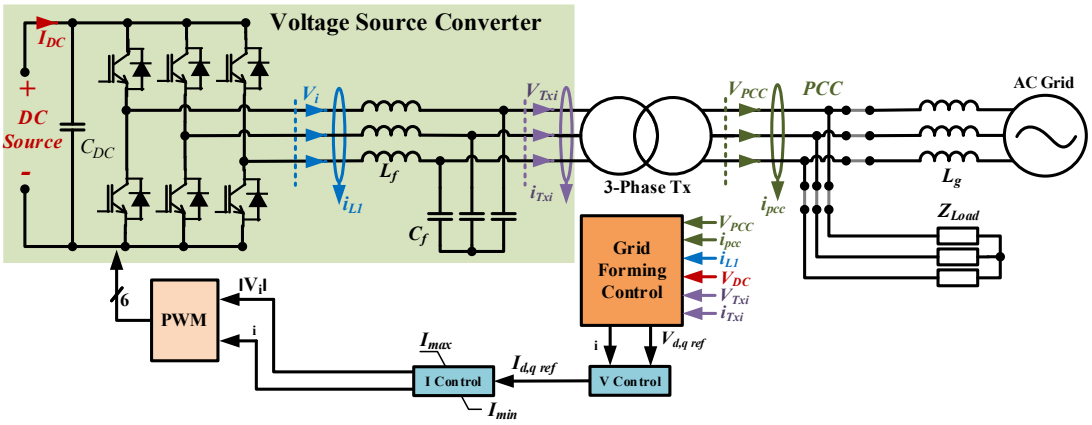

Fig. 1: High-level system diagram, consisting of grid-forming voltage source converter, a transformer, loads and the grid.

Accordingly, the contributions of this paper are summarized as:

- Proposing a modified VSM grid-forming control for black-start and grid-synchronization applications with soft black-start and improved power-based synchronization capabilities.
- Presenting a complete black-start sequence case study based on the modified controller, starting from transformer energization and load pickup to grid synchronization to demonstrate the control effectiveness.

The remaining of the paper is structured as follows: Section II provides design details of the modified VSM control. A simulation case study is presented in Section III based on the proposed GFC control design with black-start results based on the described sequence. Finally, the paper is concluded in Section IV.

II. Modified Grid-Forming Synchronizing Control

GFC controllers can vary in their level of complexity based on the application requirements. In this paper, the VSM control design is considered as a basis of the modified structure. The VSM selection is based on its direct emulation capabilities of SG inertia and damping as it stems from the swing equation [14]. Equation (1) mathematically illustrates the emulated swing equation.

$$J\frac{d\omega}{dt} = \frac{1}{\omega_{ref}}(P_{ref} - P) + D_p(\omega_{ref} - \omega) \tag{1}$$

Here, J is the virtual inertia factor, D_p is the damping factor, ω_{ref} and ω refer to the reference and measured angular frequency, with similar analogy for the active power P. This equation represents the P/f loop that generates the converter reference angle δ_i. The VSM Q/V loop is inspired from the SG analogy as in (2).

$$|V| = \omega M_f i_f \tag{2}$$

Where M_f is inspired from the mutual inductance between a SG field and stator coils, and i_f is related to the rotor excitation current. For a VSM, $M_f i_f$ is generated from the reactive power and voltage errors passed through scaling and damping coefficients as in (3).

$$M_f i_f = \int \frac{1}{K_v}(D_q\,\Delta|V| + \Delta Q)\,dt \tag{3}$$

$1/K_v$ is the integrator gain scaling factor, D_q is the voltage damping factor, $\Delta|V|$ and ΔQ are the voltage and reactive power errors, respectively.

Two VSM modifications are considered in this paper, the first replaces the typical constant voltage reference with a voltage ramp at a pre-defined rate as illustrated in (4).

$$|V_{ref}| = \begin{cases} \frac{t}{T_{ramp}}|V_{nom}| & : t < T_{ramp} \\ |V_{nom}| & : t > T_{ramp} \end{cases} \tag{4}$$

Where V_{ref} is the VSM reference voltage, V_{nom} is the nominal peak converter voltage in steady-state, t denotes time and T_{ramp} is the ramping time from 0 to 1 pu voltage. The ramping voltage reference smooths the transformer energization process and mitigates peak inrush current. The ramp definition is illustrated in Fig. 2.

The other control modification considers the grid synchronization requirement through adjusting (1) to include a temporary power term P_{sync} that is only activated when synchronization is required to influence δ_i and match it to the grid angle, resulting in (5).

$$J\frac{d\omega}{dt} = \frac{1}{\omega_{ref}}(P_{ref} - P + S_{sync}P_{sync}) + D_p(\omega_{ref} - \omega) \tag{5}$$

The switching variable S_{sync} is set to 1 only when synchronizing sequence is initiated and remains as 0 otherwise. The synchronizing power P_{sync} is the output of synchronizing control between the restarted island and the grid to drive voltage angle and frequency difference to zero. Proportional-Integral (PI) control is used to achieve this task as in (6).

$$P_{sync} = G_P\frac{\Delta\delta_{g\_pcc}}{2\pi}(K_{psync} + \frac{K_{isync}}{s}) \tag{6}$$

$\Delta\delta_{g\_pcc}$ is the angle difference between the grid voltage angle δ_g and the PCC voltage angle δ_{pcc}. Depending on the power control unit (e.g., in watts or mega-watts), the value of G_P can be set to 1 in the former case or 10^6 in the latter to limit the controller gains. K_{psync} is also defined here as a ramping

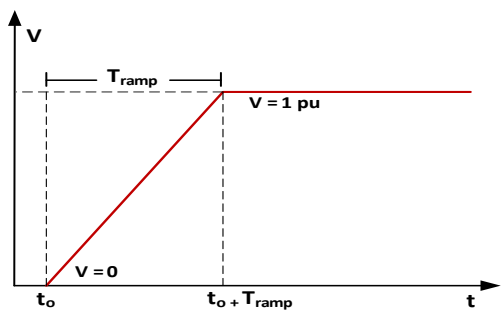

Fig. 2: Soft transformer energization voltage ramp illustration.

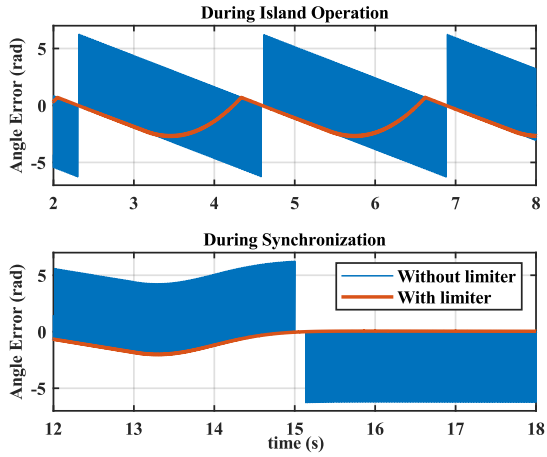

Fig. 3: Rate limiter impact on angle error (synchronization control input).

value, starting from 0 at the activation time to a design specific steady-state value in time t_{sync}. This is to avoid sudden jumps in P_{sync} to excessive values if the synchronization controller is activated at a time of high error $\Delta\delta_{g\_pcc}$.

An alternative grid synchronization design supplies the angle synchronizing controller output directly to the angle terms in (5), considering that the angular frequency is the voltage angle derivative. It has been observed through simulations that this option may require a continuously changing PI controller output as the power reference error input is typically a non-zero value. A non-zero input to the angle integrator causes the voltage angle to be in consistent looping, which leads to a moving angle that needs to be countered continuously by the controller, potentially leading to controller overflow or sudden output jumps if not accounted for properly.

On the other hand, the voltage angle and frequency signals can be extracted using a Phase-Locked-Loop (PLL) for the island PCC voltage and the grid voltage. PLL angle output is typically wrapped between 0 and 2π, this means that the angle comparator output can vary between -2π and 2π depending on which signal is leading. Instead, a rate limiter is added to extract the average angle difference value as a controller input to avoid violent variations that can negatively impact the output. The impact of using a rate limiter for $\Delta\delta_{g\_pcc}$ calculation is graphically illustrated in Fig. 3.

The controller is designed while considering grid synchronization requirements. For instance, IEEE standard as described in [15] requires that an islanded system is re-synchronized after achieving frequency, voltage and phase angle requirements. Table 1 summarizes these requirements for distribution networks up to 10 MVA.

Table 1. Typical grid sync. requirements in distribution systems.

VSC Rating	Δf (Hz)	$\Delta\lvert V\rvert$ (%)	$\Delta\delta°$
0 – 500 kVA	0.3	10	20
>500 – 1500 kVA	0.2	5	15
>1500 – 10000 kVA	0.1	3	10

Finally, the overall modified VSM controller block diagram is illustrated in Fig. 4. The synchronization task can be initiated automatically or manually by network operators when the other black-start objectives are met. Manual override switches are thus considered in the design to allow for both scenarios. Grid-forming operation mode is retained by the GFC control after synchronization with active and reactive power reference tracking.

III. Simulation Case Study

A. Simulated System Description

The case study presented in this section aims to validate the modified VSM control soft transformer energization, load pickup and grid synchronization capabilities. The system in Fig. 1 is implemented in MATLAB/Simulink. Average VSC model is used for the GFC, modified transformer saturation characteristics are selected based on combined magnitudes from literature towards the stricter saturation end. Inner voltage and current direct-quadrature (dq) vector control loops are used for protection.

The system rating is selected as 40 MVA in accordance with a MV systems case study in Scotland, the GFC output is connected to the PCC through a single-core three-phase $\Delta-\Delta$ transformer (Tx). Residual flux is set to high values to demonstrate the soft start energization effect with a 10 s duration. The overall simulated system parameters, including X/R, Short-Circuit-Ratio (SCR), VSM and inner loop control settings are summarized in Table 2. The grid synchronization requirements are defined beyond the 10 MVA values from Table 1 as the chosen system rating is higher. Thus, synchronization here can be performed after: $\Delta f < 0.1\ Hz$, $\Delta|V|$ (%) < 1%, and $\Delta\delta < 5°$ at the PCC.

The VSM P/Q references are set to $35\ MW\ (0.875\ pu)\ and\ 5\ MVAR\ (0.125\ pu)$ respectively. In this scenario, the system is activated at $t = 0$, and the VSM reference is set to ramp from 0 to 1 pu at $t = 10\ s$ for inrush current mitigation. Then, a load block of 0.5 pu (20 MW) is connected at the PCC at $t = 11\ s$ to assess the system response to load disturbance transients. The synchronization

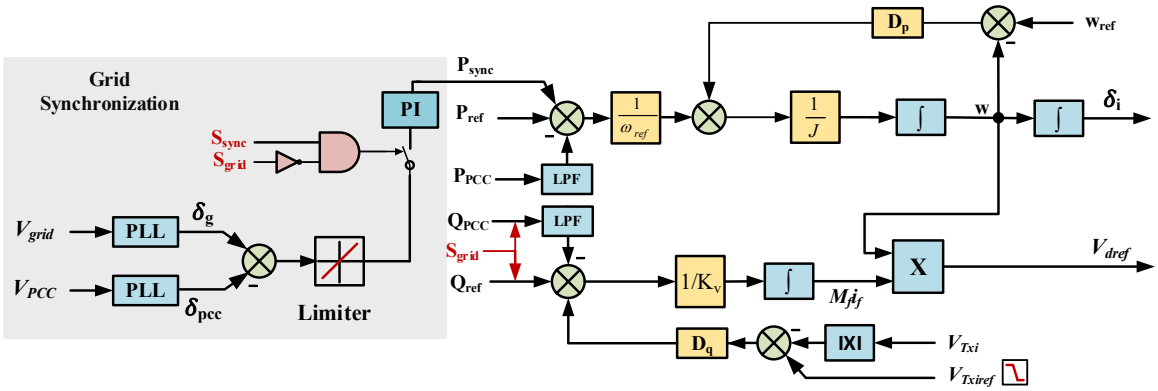

Fig. 4: Modified GFC control diagram for VSM, including the synchronization loop and transformer input ramping reference V_{Txiref}.

Table 2: Simulated Case Study Test Parameters

System Parameters ($\Delta - \Delta Tx$)			
V_{DC} (kV)	20	f_{ref} (Hz)	50
V_{Txi} (kV_{LL})	11	Grid SCR	5
V_{PCC} (kV_{LL})	33	X/R Ratio	10
S_{base} (MVA)	40	L_f (μH)	481
V_{ref} T_{ramp} (s)	10	C_f (μF)	233
Grid-Forming VSM Control Loop Parameters			
D_p	$8.106x10^4$	J	810.57
D_q	$1.781x10^5$	K_v	$5.597x10^5$
Transformer Saturation Curve (Piecewise w/ ϕ_{res} max $= 0.85\ pu$)			
$i_m(pu)$		[0, 0, 0.0024, 0.24, 1.2, 5.5]	
ϕ (pu)		[0, 0.85, 1, 1.1, 1.25, 1.4]	
$\phi_{res(a,b,c)}$ (pu)		[0 0.85 -0.85]	
Inner Vector Control Loops Parameters			
K_{pv}	0.1	K_{iv}	1
K_{pi}	9.025	K_{ii}	0.287

sequence is then initiated at $t = 13\ s$ to gradually match the voltage angles at the PCC, and finally the synchronization switch is closed. at $t = 18\ s$ after requirements are achieved.

B. Simulation Results

The observed results using the modified VSM demonstrate a successful mitigation of inrush currents, robust control response against load pickup at the PCC, and smooth transition between islanded and grid connected mode. Fig. 5(a) illustrates the minimal inrush current impact during the transformer energization segment, being limited to 0.05 pu in this case. Consequently, the reactive power is also maintained to a minimal value during transformer energization.

Initially, the deviation in active power results in a steady-state frequency deviation based on the droop factor

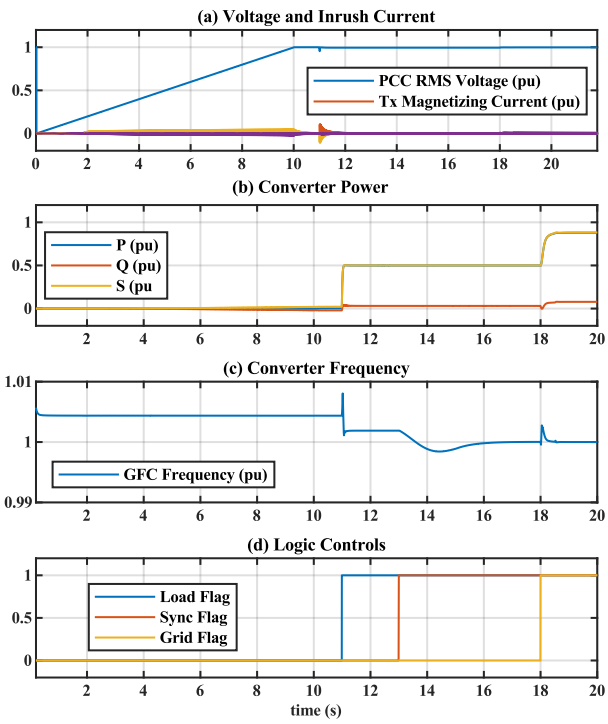

Fig. 5: Simulated case study results: (a) PCC voltage and transformer magnetizing current, (b) GFC output power, (c) VSM frequency, (d) events trigger time.

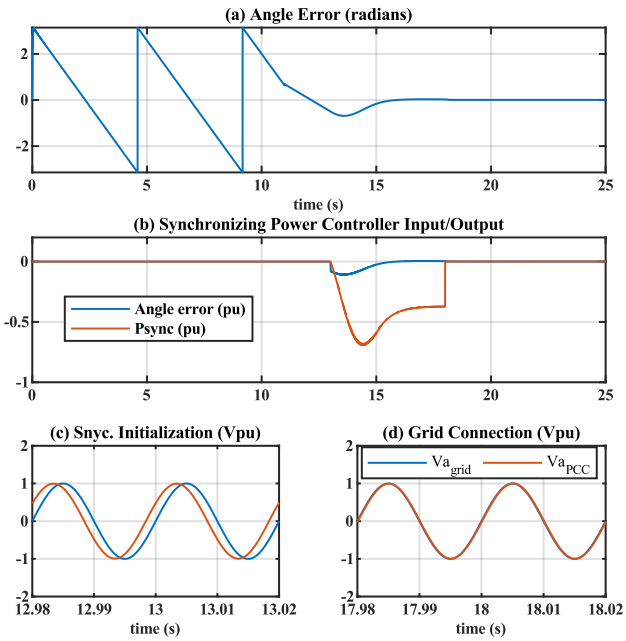

Fig. 6: Grid synchronization simulation results: (a) voltage angle error, (b) synchronizing controller input and output signal, (c) phase A voltages before synchronization, (d) phase A voltages during synchronization .

definition. The maximum deviation is designed to be 0.2 Hz and is observed between $t = 0\ and\ t = 11\ s$ until an active load is connected. This 50% rated load pickup at $t = 11\ s$ is followed by successful setpoints tracking for voltage and power quantities. Voltage angle synchronization is initiated at $t = 13\ s$, the variations in P_{sync} in Fig. 6(b) are directly reflected on the frequency in Fig. 5(c) as the controller gradually drives the steady-state angle deviation $\Delta\delta$ to zero.

As observed in Fig. 6, the angle difference is initially oscillating between $-\pi\ and\ \pi$ due to the power loop reference imbalance. After $t = 11\ s$, the angle error slope decreases as 20 MW load is connected, and the loop error reduces from 35 MW to 15 MW. Activating P_{sync} aims to drive the loop error to zero by compensating 15 MW (0.375 pu) of active power. This compensation should coincide with a zero-angle error instant, which is accounted for by the close loop controller. Given that the activation is likely to take place away from zero crossing point, the synchronizing PI proportional gain is set as a ramping value to avoid sudden jumps in P_{sync}. Namely, k_{psync} is activated at $t = 13\ s$ with a linear ramp that settles around 300 with $t_{sync} = 2\ s$. Whereas k_{isync} is set to 500.

Once the synchronization conditions are achieved, synchronization switch can be closed and seamless transition to grid-connected mode is achieved while maintaining the VSM grid-forming loop operation. The transition is activated through a manual switch at $t = 18\ s$ to allow the operator a sufficient window for conditions validation.

In grid-connected mode, the GFC power output is based on active and reactive power setpoints, and it is observed from Fig. 5(b) that $P = 0.875\ pu$ and $Q = 0.125\ pu$ are met as set by $P_{ref}\ and\ Q_{ref}$. The reactive power reference tracking path is activated after grid connection as in Fig. 5(d).

As illustrated in Fig. 7, the GFC export current is consequently increased after grid synchronization to achieve the abovementioned setpoints, while the grid current settles

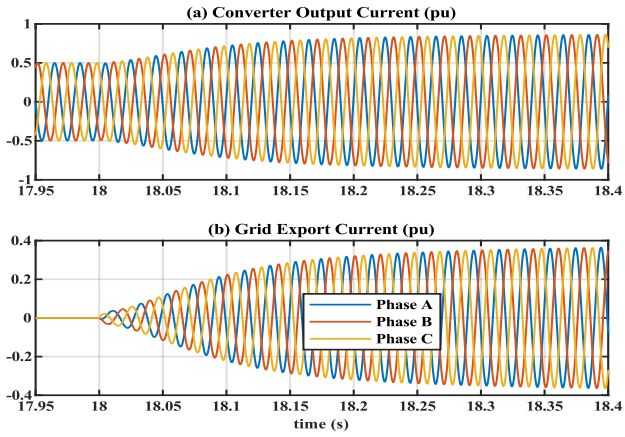

Fig. 7: Three-phase currents before and after synchronization at t = 18 s: (a) GFC output current, (b) current exported to the grid.

around 0.39 pu, accounting for the reactive power export and surplus active power beyond the local 20 MW load requirements as in equation (7).

$$\left|I_{grid(pu)}\right| = \frac{\sqrt{P_{grid}^2+Q_{grid}^2}\,V_{pcc}}{S_{base}\,V_{pcc}} \approx \frac{\sqrt{(35-20)^2+5^2}}{40} \approx 0.39\,pu \qquad (7)$$

C. Remarks

The presented analysis and simulations are based on VSM grid-forming control implementation. Soft transformer energization through ramping GFC voltage reference has been tested (with an ideal transformer assumption) by the authors in [3] using droop, PSC and matching control in addition to VSM. In principle, it is expected that these techniques should be able to achieve stable reference tracking throughout a saturable (non-ideal) transformer energization phase as presented in this paper for VSM.

The grid synchronization loop can similarly be added to the other controllers with some modifications depending on the used controller. For instance, the matching control power reference management is directly tied to DC link voltage control, and so the voltage angle synchronization with power reference adjustment may require additional considerations to maintain DC link voltage and power balance requirements.

This paper presents results based on black start from a single converter. Extending the application to multiple power-sharing converters is expected to be influenced by the converters grid-forming and grid-following combinations and droop settings. The design in such case should aim to achieve the grid synchronization requirements without jeopardizing the power sharing rules in the network.

IV. Conclusions

Grid forming converters can provide a wide range of ancillary services due to their control flexibility. This paper presented a modified GFC control based on virtual synchronous machine (VSM) control for black-start and grid-synchronization applications. The modified control uses ramping voltage reference to achieve soft transformer energization and mitigate transformer inrush currents, in addition to achieving seamless post-blackout grid synchronization by adjusting the converter power reference through a dedicated controller to match the GFC voltage angle to that of the grid. PLLs were used to extract the PCC and grid voltage angles. The synchronization controller input is filtered through a rate-limiter to smooth the controlled signal.

The proposed modified controller operation has been validated using a simulated test network with a saturable transformer to verify the inrush current mitigation capabilities. Seamless grid-connection has also been demonstrated while retaining the grid-forming operating mode after synchronization. The selection of VSM control in this paper is based on its synchronous generator analogy with virtual damping and inertia emulation parameters. The proposed GFC modifications should in principle be applicable to other techniques such as droop and PSC.

Acknowledgment

This publication is supported by Iberdrola S.A. as part of its innovation department research activities. Its contents are solely the responsibility of the authors and do not necessarily represent the official views of Iberdrola Group.

References

[1] J. Matevosyan *et al.*, "Grid-Forming Inverters: Are They the Key for High Renewable Penetration?," *IEEE Power and Energy Magazine,* vol. 17, no. 6, pp. 89-98, 2019.

[2] A. Tayyebi, D. Groß, A. Anta, F. Kupzog, and F. Dörfler, "Frequency Stability of Synchronous Machines and Grid-Forming Power Converters," *IEEE Journal of Emerging and Selected Topics in Power Electronics,* vol. 8, no. 2, pp. 1004-1018, 2020.

[3] A. Alassi, K. Ahmed, A. Egea-Alvarez, and O. Ellabban, "Performance Evaluation of Four Grid-Forming Control Techniques with Soft Black-Start Capabilities," in *2020 9th International Conference on Renewable Energy Research and Application (ICRERA)*, 27-30 Sept. 2020, pp. 221-226.

[4] D. Pan, X. Wang, F. Liu, and R. Shi, "Transient Stability of Voltage-Source Converters With Grid-Forming Control: A Design-Oriented Study," *IEEE Journal of Emerging and Selected Topics in Power Electronics,* vol. 8, no. 2, pp. 1019-1033, 2020.

[5] P. Pachore, Y. Gupta, S. Anand, S. Sarkar, P. Mathur, and P. K. Singh, "Flux Error Function Based Controlled Switching Method for Minimizing Inrush Current in 3-Phase Transformer," *IEEE Transactions on Power Delivery,* pp. 1-1, 2020.

[6] R. Ierna *et al.*, "Dispatching parameters, strategies and associated algorithm for VSM (virtual synchronous machines) and HGFC (hybrid grid forming convertors) ," 2019.

[7] S. McGuinness *et al.*, "Coordination of AC protection settings during energisation of AC grid from a VSC HVDC interconnector," *15th International Conference on Developments in Power System Protection (DPSP 2020),* Liverpool, UK, 2020, pp. 1-6.

[8] A. Roscoe *et al.*, "Practical Experience of Providing Enhanced Grid Forming Services from an Onshore Wind Park," 2019.

[9] J. Wang, B. Lundstrom, and A. Bernstein, "Design of a Non-PLL Grid-forming Inverter for Smooth Microgrid Transition Operation," in *2020 IEEE PESGM 2020*, 2-6 Aug. 2020, pp. 1-5.

[10] J. Wang, A. Pratt, and M. Baggu, "Integrated Synchronization Control of Grid-Forming Inverters for Smooth Microgrid Transition," in *2019 IEEE Power & Energy Society General Meeting (PESGM)*, 4-8 Aug. 2019, pp. 1-5.

[11] C. Lee, R. Jiang, and P. Cheng, "A Grid Synchronization Method for Droop-Controlled Distributed Energy Resource Converters," *IEEE Trans. on Industry Applications,* vol. 49, no. 2, pp. 954-962, 2013.

[12] A. Alassi *et al.*"HVDC Transmission: Technology Review, Market Trends and Future Outlook," *Renewable and Sustainable Energy Reviews,* vol. 112, pp. 530-554, 2019.

[13] "Distributed ReStart: Power Engineering and Trials - Power Systems Studies Part 1," National Grid ESO, UK, 2020.

[14] Q. Zhong and G. Weiss, "Synchronverters: Inverters That Mimic Synchronous Generators," *IEEE Transactions on Industrial Electronics,* vol. 58, no. 4, pp. 1259-1267, 2011.

[15] M. Ashabani, F. D. Freijedo, S. Golestan, and J. M. Guerrero, "Inducverters: PLL-Less Converters With Auto-Synchronization and Emulated Inertia Capability," *IEEE Transactions on Smart Grid,* vol. 7, no. 3, pp. 1660-1674, 2016.